Preparation and characterization of microporous PVDF membrane by thermally induced phase separation from a ternary polymer/solvent/non-solvent system

Min Liu[a,b], Zhen-liang Xu[a,b*], Dong-gen Chen[a], Yong-ming Wei[a]

[a]*Membrane Science and Engineering R & D Lab, Chemical Engineering Research Center, East China University of Science and Technology (ECUST), 130 Meilong Road, Shanghai 200237, China*
Tel. +862164252989; Fax +862164252989; email: chemxuzl@eucst.edu.cn; liumin@ecust.edu.cn
[b]*Shanghai Key Laboratory of Advanced Polymeric Materials, Key Laboratory for Ultrafine Materials of Ministry of Education, School of Materials Science and Engineering, ECUST, 130 Meilong Road, Shanghai 200237, China*

ABSTRACT

Porous poly(vinylidene fluoride) (PVDF) microporous membranes were successfully prepared from a ternary system including PVDF, solvent and non-solvent via thermally induced phase separation (TIPS) process. Tributyl citrate (TBC) as solvent and di-(2-ethylhexyl) phthalate (DEHP) as non-solvent were used in this study. The effect of mixed diluent composition on PVDF/TBC/DEHP system phase diagram was studied. Phase separation mechanism changed from solid–liquid phase separation to liquid–liquid phase separation with the increase content of non-solvent DEHP. Effects of mixed diluent composition, polymer concentration, cooling condition on morphology, water permeability, porosity and pore size were studied. The membranes which formation controlled by L–L phase separation mechanism have narrow pore size. For the system of 30 wt/70 wt TBC/DEHP with L–L phase separation, bi-continuous morphology was observed. For the system of 90 wt/10 wt TBC/DEHP with S–L phase separation, spherulites structure was obtained. With the polymer concentration increased, the values of porosity, pure water permeability flux and mean pore radius all decreased. For the same polymer content, the membranes prepared from 30 wt/70 wt TBC/DEHP system have better performance. Membranes possessed nice performance prepared in the 20°C water bath.

Keywords: Poly(vinylidene fluoride); Thermally induced phase separation; membranes; Morphology; L–L phase separation

1. Introduction

The thermally induced phase separation (TIPS) process was first introduced by Castro [1] in early 1980s. In TIPS process, a polymer was dissolved in a diluent at a high temperature, and a homogenous polymer/diluent solution is obtained. By lowering the temperature of the solution, liquid–liquid (L–L) phase separation and solid–liquid (S–L) phase separation can occur respectively or simultaneously. Subsequently diluent was extracted to produce membrane structure.

In 1990s, Lloyd et al. [2–7] researched the TIPS mechanisms and investigated the effect of thermodynamic interaction, cooling condition, characteristics of diluent and crystallization kinetics on the isotactic polypropylene (iPP) membrane morphology in detail.

*Corresponding author

In early 2000s, Matsuyama team worker [8–14] succeed in preparing iPP, poly(ethylene-co-vinyl(alcohol) (EVOH), poly(vinylidene fluoride) (PVDF), polyethylene (PE) and polyvinyl butyral (PVB) microporous membranes.

During the TIPS process, it undergoes L–L or S–L phase separation which mainly depending on the polymer–diluent interaction, polymer content, and the cooling depth (between the solution temperature and the quenching temperature). The final morphology of membrane depends on the kinetics as well as thermodynamics of the phase separation. If the polymer–diluent interaction is strong, S–L phase separation occurs, which lead to the formation of spherulitic microstructure morphology at any polymer concentration [15]. If the polymer–diluent interaction is weak but still have compatibility at high temperature, a bi-continuous morphology was formed which usually due to L–L phase separation at a low polymer concentration [16]. But it is difficult to find a single diluent which could dissolve the polymer at high temperature meanwhile could undergoes L–L phase separation at high polymer concentration. Therefore, in order to control the polymer–diluent interaction, a ternary polymer/solvent/non-solvent system was applied, which adjust the compatibility between polymer and diluent through changing the ratio of solvent and non-solvent. It is definitely that this is a convenient, practical, and perspective method in membrane industry.

Some studies have been reported on the PVDF membranes formation via TIPS. But most of the interests were focused on the polymer solutions with single diluent [15,16]. But few works [14,17,18] have reported about the systems with mixed diluents, such as mixtures of triacetin with glycerol, dibutyl phthalate (DBP) with di(2-ethylhexyl) phthalate (DEHP). As an environment friendly solvent, tributyl citrate (TBC) can be considered as diluent for PVDF because of its innocuity, insipidity, high boiling point, non-volatility, thermostability, good chemical stability and good compatibility with many kinds of polymers. Thereby, conventional phthalate was gradually substituted by citrate nowadays. However, no such study has so far been carried out to analyze TBC influence on membrane morphology and structure. In view of only spherulitic microstructure was gained with single diluent of TBC in our early research, the aim of this research is to prepare porous PVDF membrane via TIPS method with diluent mixtures of TBC (solvent) and DEHP (non-solvent).

The phase diagram of PVDF/TBC/DEHP was determined. The effects of mixed diluent composition on membranes morphology was studied by scanning electron microscopy (SEM). In addition, the effects of the polymer concentration and cooling condition on the membrane morphology and performances were examined detailed.

2. Experiment

2.1. Materials

PVDF (Solef 6010, = 166,000, M_w/M_n = 1.7) was supplied with Solvay (France). TBC (density = 1.039 g/cm^3, boiling point = 170°C(at 133.3 Pa), DEHP (density = 0.983 g/cm^3, boiling point = 386°C) and ethanol were purchased from Shanghai Chemical Reagent Co. The ethanol and hexane used as extraction solvent. All chemicals were used without purification.

2.2. Preparation of the PVDF/TBC/DEHP systems and membranes

A mixture of several certain ratios of two diluents (TBC, DEHP) was premixed. PVDF and the mixed diluent were weighed to a glass vessel with stirrer (if the PVDF concentration was high, stirrer was unable, the blends were periodically agitated manually) for at least 1 h at 200°C to formed a homogeneous solution. Then the systems quenched in ice water to be solidified, and the blend materials were used for cloud point tests, crystallization temperature measurements, and the preparation of membranes.

There are two methods for the preparation of membranes. First, the solidified blend samples were sliced into small pieces, melted again to obtain homogeneous PVDF/TBC/DEHP solution. The solution was cast onto alloyed plate at 220°C by means of a casting knife with a gap of 350 μm, and then quenching quickly. Secondly, the solidified blend samples were sliced into small pieces, placed between two microscope coverslips. The membrane thickness was controlled by the insertion of Teflon film (200 μm) between the slips. Then the sample was heated at 220°C for 2 min on the hot stage and solidified by quenching at different cooling condition. The diluent in the membrane was extracted by ethanol for 48 h; subsequently ethanol was extracted by hexane. Finally, the membrane dried in open air to remove hexane at least two days.

2.3. Phase diagram

The cloud point (T_{cloud}) was measured according to the method reported by Lloyd et al. [3]. The light transmittance measurement experiments were carried out by a self-made device schematically was shown in Fig. 1. In the method, the small pieces sample was
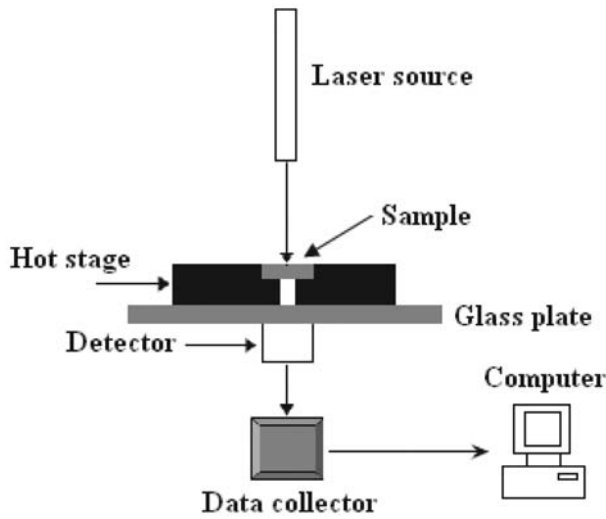
Fig. 1. Schematics of light transmission device.

placed between two microscope coverslips. A Teflon film with a small opening in the center and vacuum grease were inserted between the coverslips. The coverslip assembly containing the blends was heated on a hot stage (KEL-XMT-3100) to 220°C at 10°C/min and held at for 3 min to assure homogeneity of the melt. Light was passed through the sample and the intensity of the transmitted light was captured by the light detector and then recorded as the temperature of the sample was decreased at 10°C/min to 50°C. The experiment was conducted with collimated laser. The intensity of the transmittance light decreased as the liquid–liquid phase separation occurred. The onset of the signal change was used as an indication of the onset of the liquid–liquid phase separation.

The crystallization temperature (T_c) was determined with differential scanning calorimeter (DSC, MDSC2910, TA Co.). All measurements were performed under nitrogen atmosphere, and the sample weights about 8 mg. The blends was sealed in an aluminum DSC pan, melted, and kept at 200°C for 5 min to erase thermal history and ensure complete melting; it was then cooled at 10°C/min to 50°C, and then heated to 200°C at 10°C/min. The onset of the exothermic peak was taken as the T_c. The onset of the endothermic peak during the second heating was taken as melting temperature (T_m).

2.4. Membrane performances characterization

PVDF microporous membranes were characterized by the determination of pure water permeability flux (PWP), porosity (ϵ), minimum bubble point pressure, and mean pore radius (r_m). A self-made dead-end stirred cell (effective area 11.34 cm^2) was used to measure the PWP flux of the PVDF membranes. The PWP flux is defined as:

$$PWP = Q/(AT), \tag{1}$$

where Q is the volume of permeate pure water (L), A is the effective area of the membrane (m^2), and T is the permeation time (h).

The porosity was determined by gravimetric method, defined as:

$$\varepsilon = \frac{(m_1 - m_2)/\rho_{ethanol}}{(m_1 - m_2)/\rho_{ethanol} + m_2/\rho_p}, \tag{2}$$

where m_1 is the weight of the wet membrane; m_2 is the weight of the dry membrane; $\rho_{ethanol}$ is the ethanol density (0.790 g·cm^{-3}); ρ_P is the polymer density (1.780 g·cm^{-3}).

Mean pore radius was determined by filtration velocity method. According to Guerout–Elford–Ferry equation [19], r_m could be calculated:

$$r_m = \sqrt{(2.9 - 1.75\varepsilon)8\eta hQ/\varepsilon A\Delta P}, \tag{3}$$

where η is water viscosity (8.9×10^4 Pa·s); h is the membrane thickness (m); ΔP is the operation pressure (0.1 MPa).

Maximum pore size can be characterized by bubble point procedure. The bubble point is a determination of the minimum pressure (bubble point) at which a wetting liquid is pressed out of the pore system of a membrane while forming a steady bubble chain, and is also a common method of determining the maximum pre size. Bubble point pressure is determined by a DJ-5 membrane bubble point testing instrument (maximum input pressure ≤ 0.6 MPa) produced by Shanghai Eling filter equipment Co., Ltd (China). Membrane was immersed in ethanol at least for 3 h and fitted on the testing instrument. Then bubble point pressure can be obtained automatically. According to Laplace's equation, maximum pore size could be calculated:

$$R_{max} = 2\sigma \cos\theta/P, \tag{4}$$

where σ is the surface tension of ethanol (23.0×10^{-3} N·m^{-1}); θ is the contact angle of ethanol to membrane; P is the minimum bubble point pressure.

2.5. Morphology characterization of the membrane

The microporous membrane was fractured in liquid nitrogen. The surface and cross-section of the membrane were sputter-coated with gold. Then the
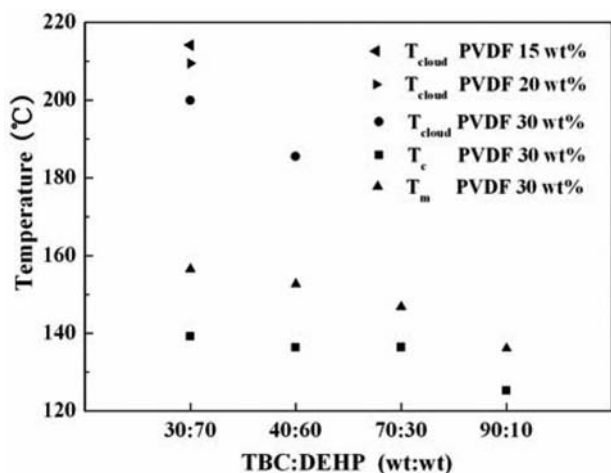
Fig. 2. Phase diagram of PVDF/TBC/DEHP system.

morphologies of the membranes were observed with SEM (JEOL Model JSM -6360LV, Japan).

3. Results and discussion

3.1. Phase diagram

The phase diagram for the PVDF/TBC/DEHP system, shown in Fig. 2, displays the effects of the mixed diluent composition and the polymer concentration on the phase diagram. When PVDF concentration was fixed at 30 wt% and TBC/DEHP ratio was changed, cloud point (T_{cloud}) was observed with 40 wt/60 wt and 30 wt/70 wt TBC/DEHP, which means the existence of the liquid–liquid (L–L) phase separation. The T_{cloud} appeared and shift to a high temperature with the DEHP content increasing. Meanwhile, the crystallization temperature (T_c) changed a little. This means the area between the binodal line and crystallization line becomes larger. As shown in Fig. 2, it was found that the T_m moved to high temperature as the DEHP content increasing. But the temperature changes of T_{cloud} were more sensitive than that of T_c and T_m. On the other hand, T_{cloud} decreased with the PVDF concentration increasing by 30 wt/70 wt TBC/DEHP fixed. Thus, only the T_c was observed with 70 wt/30 wt and 90 wt/10 wt TBC/DEHP, which means only the solid–liquid (S–L) phase separation. And, the T_c of sample with 90 wt/10 wt TBC/DEHP is less than that of pure PVDF ($T_c = 138°C$) significantly. It is consonant with melting point depression theory [2].

To explain the phase separation behavior of the sample, the blend system's was useful. If there is good compatibility between polymer and mixed diluent, i.e., strong polymer–diluent interaction, phase separation mechanism goes through S–L phase separation, such as the 90 wt/10 wt TBC/DEHP system. To the contrary, L–L phase separation takes place, such as the 30 wt/70 wt TBC/DEHP system. Without a doubt, the compatibility changes worse as the DEHP content increased.

3.2. Effect of mixed diluent composition on the membrane morphology

By varying the weight fraction of TBC in the mixed diluent systematically, microporous membranes with different morphology were obtained via TIPS. The micrographs of cross-section are shown in Fig. 3. As described above, the formation of spherulites governed by crystallization mechanism was found throughout the membrane in the M1 and M2 membranes. As clearly shown in Fig. 3 (M3, M4), bi-continuous structure, brought about from L–L phase separation, was formed in a thin layer near the upper surface of the membrane meanwhile irregular spherulitic particles structure were observed at the other parts of the membrane. This phenomenon was due to different cooling rate of the membrane at the upper and bottom surface of the membrane. The cooling rate was quickly because of the direct contact of hot polymer solution with quench bath, the cooling rate at the bottom surface was low due to the contact of polymer solution with quench bath through hot alloy plate. The higher cooling rate means the possibility of crystallization is little. Therefore bi-continuous structure by L–L phase separation was clearly observed only near the upper surface of the membrane.

3.3. Effect of PVDF concentration on the membrane morphology

The effect of polymer concentration on the cross section morphology of membranes is shown in Figs. 4 and 5. First, as shown in Fig. 4, the system with mixed diluent of 30 wt/70 wt TBC/DEHP was researched. When the polymer concentration increased from 20 to 60 wt%, the bi-continuous morphology was observed in all concentration, although some crystallites are existed other than 30 wt %, but no large spherulites were found. Other, in Fig. 4 (M8), the connectivity of the pores was lower than other three membranes. This maybe the higher polymer concentration led to higher viscosity that restrained the rate of phase separation and the porosity of membrane. Second, the system with the mixed diluent of 90 wt/10 wt TBC/DEHP was shown in Fig. 5. The spherulites structure was obtained in all concentration. The spherulites size became larger and packing denser, and the pore volume between
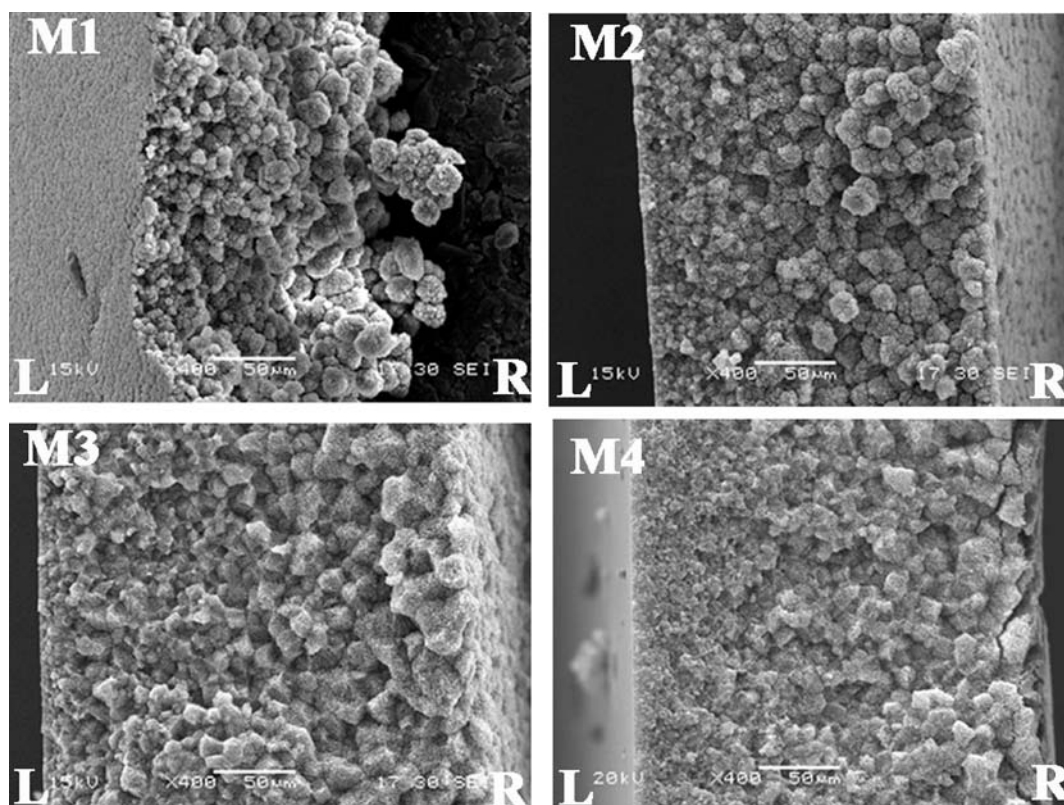
Fig. 3. SEM images of cross-section of membranes with 30 wt% PVDF. TBC/DEHP wt/wt: (M1) 90:10; (M2) 70:30; (M3) 40:60; (M4) 30:70; Cooling condition: ice water; L: upper side, R: bottom side.

spherulites was also decreased with the polymer concentration increased. This may be ascribed to the influence of viscosity. High polymer content will lead to higher viscosity, which in turn prevented PVDF from crystallizing during TIPS process.

The above change in the membrane morphology accounts for the different phase separation mechanism. For the membrane in Fig. 4, bi-continuous structure was formed because of the L–L phase separation. For the membrane in Fig. 5, spherulites structure was obtained because of the S–L phase separation.

3.4. Effect of cooling condition on the membrane morphology

The morphology of membrane with two different cooling conditions was shown in Fig. 6. In the case of water at 20°C cooling condition, more homogenous surface and cross section structure was gained. For a semi-crystalline polymer, L–L phase separation is accompanied by polymer crystallization, either simultaneously or subsequently [20]. In the cooling condition of ice water, the high temperature polymer solution quenched to 0°C directly, the blend systems went through the L–L phase separation area quickly and arrived at the crystallization line. As a result, the

mainly factor of membrane forming mechanism is the crystallization. So surface structure was uneven, the cross section was asymmetric. Thus in the cooling condition of water at 20°C, although the super-cooling depth (between the solution temperature and the quenching temperature) is lower than in the ice water, but enough to depressed the polymer crystallization, which means the high temperature polymer solution experience more time of the L–L phase separation region. As a result of the competition between L–L phase separation and crystallization, the L–L phase separation is predominant.

3.5. Performance of membrane

The effect of mixed diluent composition on the membranes performances was shown in Table 1. At the same polymer concentration and cooling condition, with non-solvent DEHP content increase, the mean pore radius (r_m), PWP and maximum pore size (R_{max}) decreased. The porosity was a little increase, but approximately the same. The M1-b and M2-b membranes, which controlled by S–L phase separation mechanism, have bigger r_m, R_{max} and larger PWP that mainly due to micropores between spherulites. To the
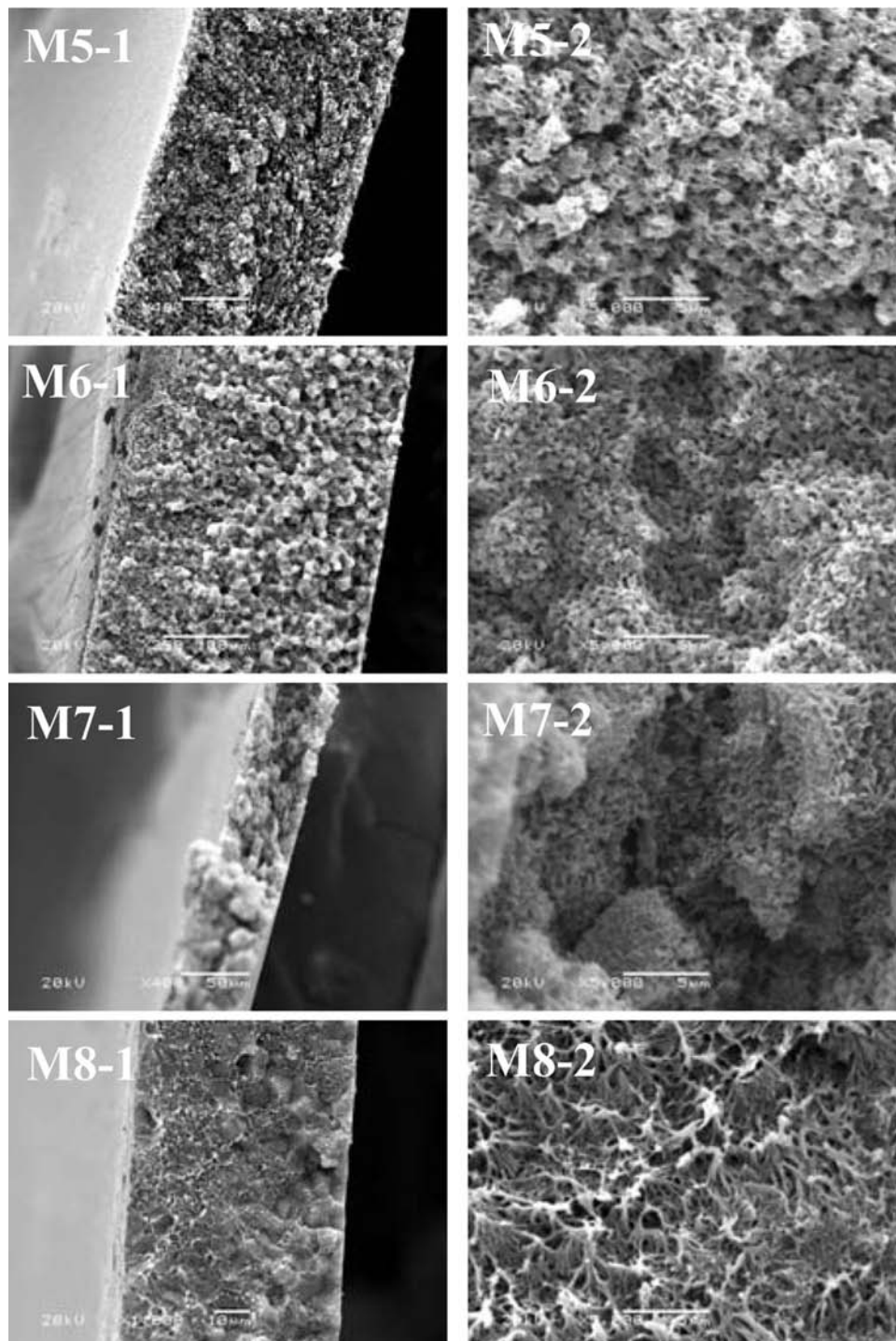
Fig. 4. SEM images of the membranes. Cooling condition: water at 20°C. 30 wt/70 wt TBC/DEHP, PVDF concentration: (M5) 20; (M6) 30; (M7) 40; (M8) 60wt%. 1: whole cross section; 2: enlarge cross section.

contrary, M3-b and M4-b membranes, which controlled by L–L phase separation mechanism, have lower ratio of r_m to R_{max} that means better homogenous pore size. The difference between the porosity of different mixed composition may be the different phase separation mechanisms. As described above, the M1-b prepared in S–L phase separation membrane formation condition, while the M4-b prepared in L–L phase separation, which is favorable to obtain the higher porosity.
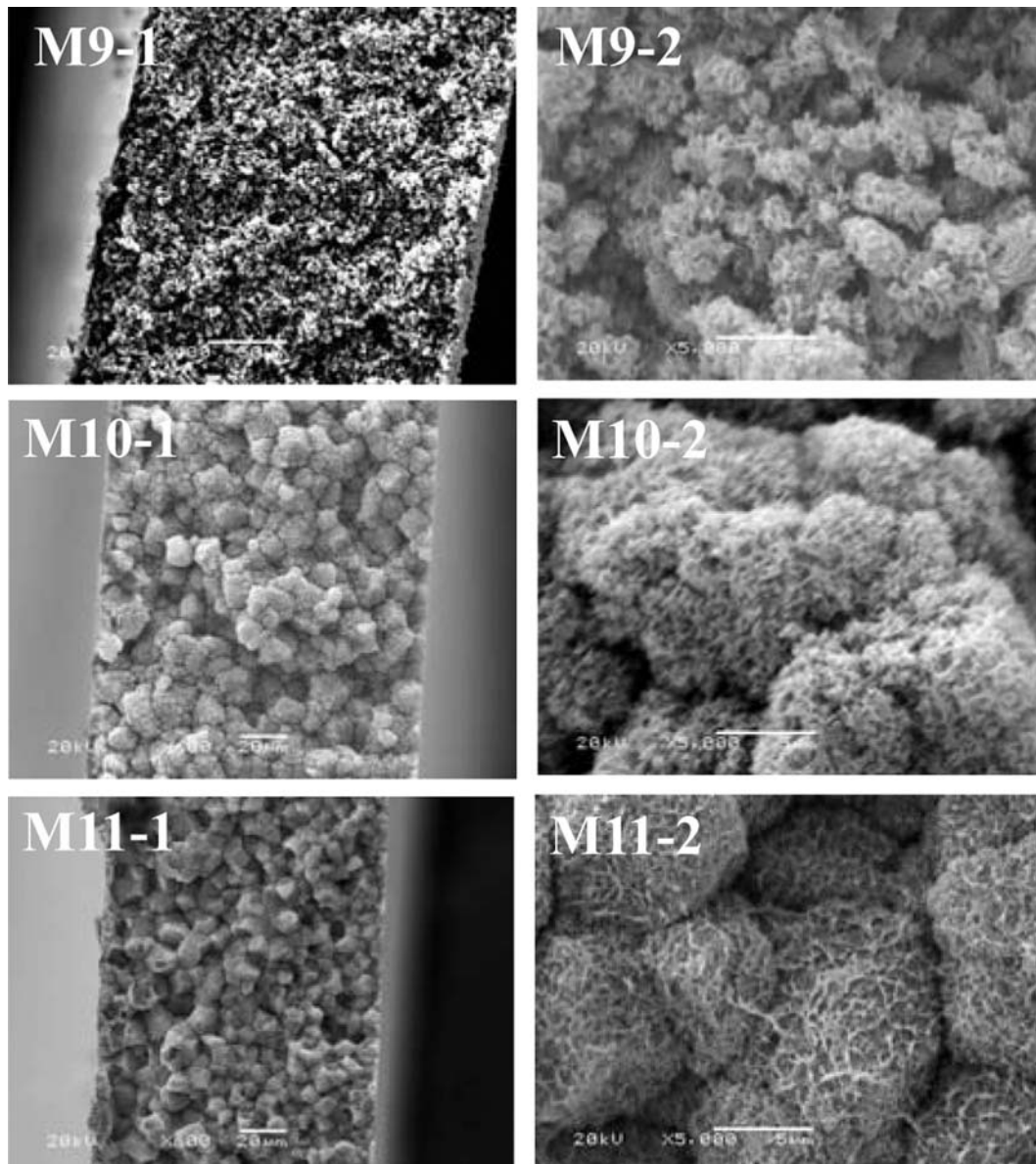
Fig. 5. SEM images of the membranes. Cooling condition: water at 20°C. 90 wt/10 wt TBC/DEHP, PVDF concentration: (M5) 30; (M6) 40; (M7) 60 wt%. 1: whole cross section; 2: enlarge cross section.

The effect of polymer concentration on the membrane performances was shown in Table 2. First, either 30 wt/70 wt or 90 wt/10 wt TBC/DEHP systems, with the polymer concentration increased, the values of porosity, PWP and r_m all decreased. Porosity comes from the space occupied by diluent, with the polymer concentration increased, the diluent content decreased accordingly. As a result, the above performances must be decreased. Second, for the same polymer content (such as 30 wt% PVDF) and different mass ratio of TBC/DEHP, although 90 wt/10 wt TBC/DEHP system has higher PWP which maybe mainly due to the higher R_{max}, but 30 wt/70 wt TBC/DEHP system has higher

porosity, lower R_{max} and r_m. This means membranes prepared from L–L phase separation systems have narrower pore size distribution. From the ratio of R_{max}/r_m (2.62<6.33) also can conclude. Besides, at the 40 wt% PVDF, membrane prepared from 30 wt/70 wt TBC/DEHP system significantly have higher PWP and r_m which shown the advantages of L–L phase separation.

The value of porosity, PWP and pore size of membranes prepared from different cooling condition shown in Table 3. The case of water at 20°C cooling condition, the R_{max} was 0.157 μm lower than that of 0.482 μm, and value of R_{max}/r_m is only 2.62. These results further confirmed the research conclusion
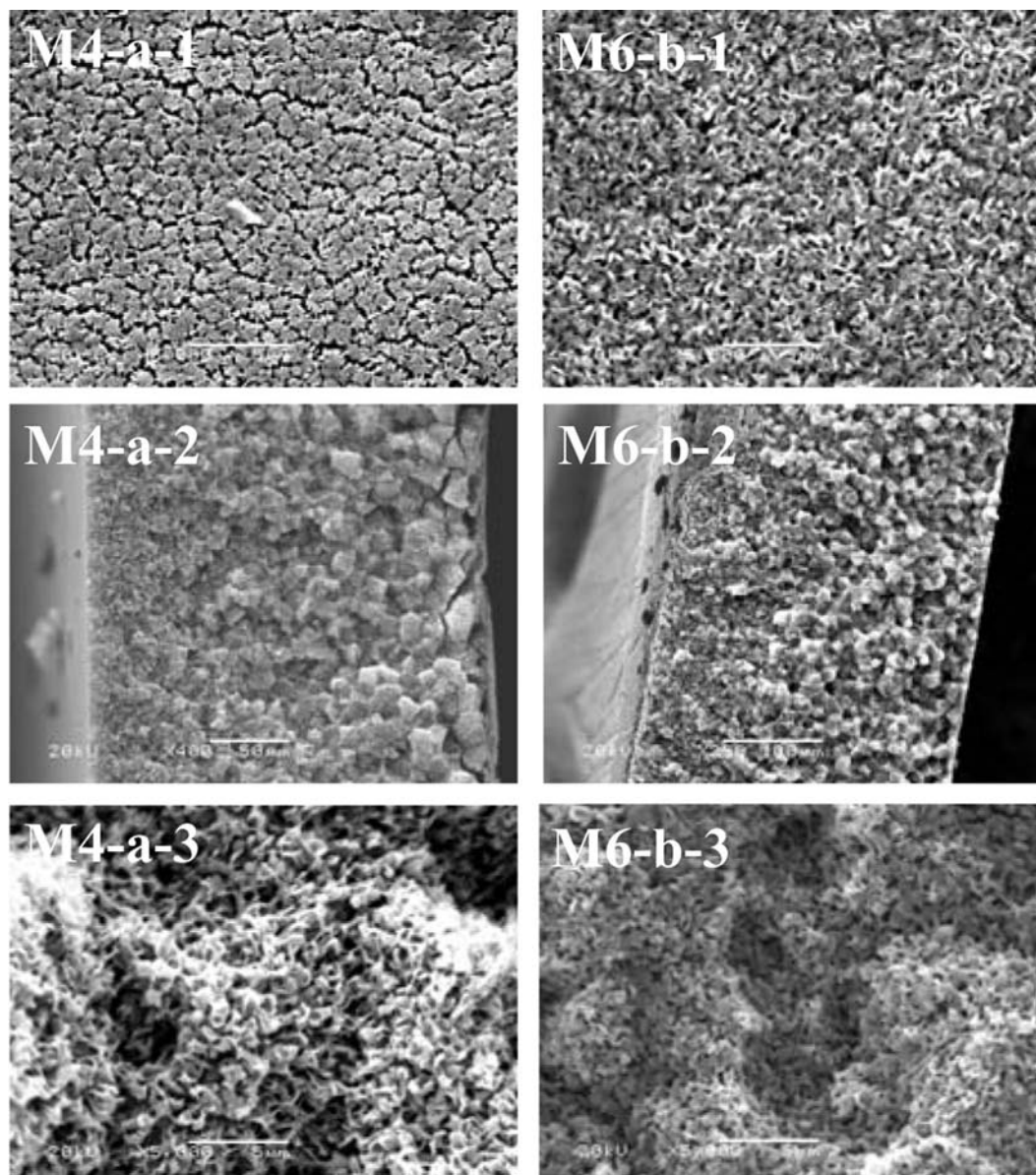
Fig. 6. SEM images of two membranes prepared at different cooling conditions. (a) ice-water; (b) water at 20°C; PVDF concentration: 30 wt%; 1: upper surface; 2: whole cross-section; 3: enlarge cross section (near the upper surface).

Table 1
Effect of mixed diluent composition on the membrane performance

Number	TBC/DEHP (wt/wt)	PWP (L m^{-2} h^{-1})	Porosity (ε)	R_{max}/r_m	Pore size	
					r_m (µm)	R_{max} (µm)
M1-b	90:10	477	0.756	6.33	0.082	0.519
M2-b	70:30	336	0.775	3.30	0.063	0.208
M3-b	60:40	326	0.775	2.51	0.061	0.153
M4-b	30:70	235	0.783	2.62	0.060	0.157

Note: b: cooling bath: water at 20°C; PVDF concentration: 30 wt%.

Table 2
Effect of polymer concentration on the membrane performance

TBC/DEHP (wt/wt)	PVDF (wt %)	PWP (L m^{-2} h^{-1})	Porosity (ε)	R_{max}/r_m	Pore size	
					r_m (μm)	R_{max} (μm)
30:70	30	235	0.783	2.62	0.060	0.157
30:70	40	116	0.679	9.67	0.058	0.561
30:70	60	4	0.537	29.5	0.012	0.354
90:10	20	∞	0.850	–	–	3.195
90:10	30	477	0.756	6.33	0.082	0.519
90:10	40	23	0.708	26.25	0.024	0.630

Note: cooling bath: water at 20°C; ∞: infinitely-great.

Table 3
Effect of cooling condition on the membrane performance

TBC/DEHP (wt/wt)	Cooling condition	PWP (L m^{-2} h^{-1})	Porosity (ε)	R_{max}/r_m	Pore size	
					r_m (μm)	R_{max} (μm)
30:70	ice water	300	0.805	7.42	0.065	0.482
30:70	20°Cwater	235	0.783	2.62	0.060	0.157

Note: PVDF concentration: 30 wt%.

described above in Fig. 6. The membrane with the better performance prepared in this study is in the 20°C water bath.

4. Conclusion

Phase diagram for the PVDF/TBC/DEHP system were determined. Cloud point was appeared and shift to higher temperature with the increase content of non-solvent DEHP, while crystallization temperature changed a little. This means membrane formation mechanism could control by adjust the ratio of solvent and non-solvent easily.

The effect of mixed diluent composition, polymer concentration and cooling condition on the membrane structures and performance were researched. When the polymer concentration was fixed 30 wt%, bi-continuous morphology was gained from the M3 and M4. And with non-solvent DEHP content increase, mean pore radius, PWP flux and maximum pore size decreased. The membranes which formation controlled by L–L phase separation mechanism have narrow pore size. For the system of 30 wt/70 wt TBC/DEHP with L–L phase separation, bi-continuous morphology were observed with the polymer concentration increase from 20 to 60 wt%. For the system of 90wt/10wt TBC/DEHP with S–L phase separation, spherulites structure was obtained, and spherulites size increased

and impinged dense with the polymer concentration increase from 20 to 40 wt%. Either 30 wt/70 wt or 90 wt/10 wt TBC/DEHP systems, with the polymer concentration increased, the values of porosity, pure water penetration flux and mean pore radius all decreased. For the same polymer content, the membranes prepared from 30 wt/70 wt TBC/DEHP system have better performance. In additional, membranes with the better performances were prepared in the 20°C water bath. In one word, if want to obtain different porous structures, there are still many research works which should be done in the future.

Symbols

Q	volume of permeate pure water (L)
A	effective area of membrane (m^2)
T	permeation time (h)
PWP	pure water permeability flux (L·m^{-2}·h^{-1})
ϵ	porosity

m_1	weight of the wet membrane (g)
m_2	weight of the dry membrane (g)
$\rho_{ethanol}$	ethanol density (g·cm^{-3})
ρ_P	polymer density (g·cm^{-3})
r_m	mean pore radius (μm)
η	water viscosity (Pa·s)
h	membrane thickness (μm)
ΔP	operation pressure (MPa)
R_{max}	maximum pore size (μm)
σ	surface tension of ethanol (N·m^{-1})
θ	contact angle of ethanol to membrane (°)
P	minimum bubble point pressure (MPa)

References

[1] A.J. Castro, U.S. Patent 4 247 498, 1981.
[2] D.R. Lloyd, K.E. Kinzer and H.S. Tseng, J. Membr. Sci., 152 (1990) 239–261.
[3] D.R. Lloyd, S.S. Kim and K.E. Kinzer, J. Membr. Sci., 64 (1991) 1–11.
[4] S.S. Kim and D.R. Lloyd, J. Membr. Sci., 64 (1991) 13–29.
[5] G.B.A. Lim, S.S. Kim, Q.H. Ye, et al., J. Membr. Sci., 64 (1991) 31–40.
[6] S.S. Kim, G.B.A. Lim, A.A. Alwattari, et al, J. Membr. Sci., 64 (1991) 41–53.
[7] A.A. Alwattari and D.R. Lloyd, J. Membr. Sci., 64 (1991) 55–68.
[8] H. Matsuyama, M. Terarnoto and S. Kudari, J. Appl. Polym. Sci., 82 (2001) 169–177.
[9] H. Matsuyama, M. Taisuke, T. Masaaki, et al., J. Membr. Sci., 204 (2002) 323–328.
[10] H. Matsuyama, H. Okafuji and M. Taisuke, J. Membr. Sci., 223 (2003) 119–126.
[11] H. Matsuyama, H. Kentarou, M. Taisuke, et al., J. Appl. Polym. Sci., 93 (2004) 471–474.
[12] H. Matsuyama, T. Iwatani, Y. Kitamura, et a1, J. Appl. Polym. Sci., 79 (2001) 2449–2455.
[13] X.Y. Fu, H. Matsuyama, M. Teramoto, et al, Sep. Purif. Technol., 45 (2005) 200–207.
[14] S. Rajabzadeh, T. Maruyama, T. Sotani and H. Matsuyama, Sep. Purif. Technol., 63 (2008) 415–423.
[15] M.H. Gu, J. Zhang, X.L. Wang, H.J. Tao, et al, Desalination, 192 (2006) 160–167.
[16] Z.Y. Cui, C.H. Du, Y.Y. Xu, et al, J. Appl. Polym. Sci., 108 (2008) 272–280.
[17] G.L. Ji, C.H. Du, B.K. Zhu, et al, J. Appl. Polym. Sci., 105 (2007) 1496–1502.
[18] G.L. Ji, B.K. Zhu, C.F.Zhang, et al, J. Appl. Polym. Sci., 107 (2008) 2109–2117.
[19] C.S. Feng, B.L. Shi, G.M. Li, et al, J. Membr. Sci., 237 (2004) 15.
[20] J. Yang, D.W. Li, Y.K. Lin, et al, J. Appl. Polym. Sci., 110 (2008) 341–347.